Properties of Interdigital Transducers for Lamb-Wave Based SHM Systems

M. MANKA[1], M. ROSIEK[1], A. MARTOWICZ[1], T. UHL[1]
and T. STEPINSKI[2]

ABSTRACT

Recently, an intensive research activity has been observed concerning the application of guided waves to long range ultrasound (LRUT) and structural health monitoring. Guided waves propagating in plates, known as Lamb waves, have appeared to be suitable for monitoring and condition evaluation of planar structures. Lamb waves can be generated using different types of actuators including piezoelectric or electromagnetic acoustic transducers. In this paper a novel type of piezoelectric transducers is presented based on macro-fiber piezocomposite (MFC). Contrary to the previously presented MFC transducers the transducers presented here are provided with interdigital electrodes matched to certain wavelength. Two different designs of interdigital transducers (IDT) made of MFC substrate are presented in the paper together with the results of numerical simulations and experimental tests.

INTRODUCTION

Applications of guided ultrasonic waves to nondestructive testing (NDT) and structural health monitoring (SHM) have been intensively increasing during the past decades [1]. One type of guided waves that is particularly useful in SHM applications are plate ultrasonic waves. This type of waves can propagate in thin plates with parallel free boundaries. The main advantage of the plate waves, also called Lamb waves, is that they may travel over a long distance in different types of materials including materials characterized by a high attenuation (i.e.: carbon fiber composites) [2]. Lamb waves allow for monitoring of large areas with a few actuators/sensors only [3,4,5]. Moreover, Lamb waves allow for the examination of entire cross section of a planar structure and they are sensitive for different types of defects [6].

Among the transducers that may be used for the generation of Lamb waves interdigital transducers (IDT) are gaining an increasing recognition.

[1] AGH University of Science and Technology Department of Robotics and Mechatronics, Al. Mickiewicza 30, 30-059 Krakow, Poland
[2] Signals and Systems, Uppsala Universitet, P.O. Box 534, SE-751 21 Uppsala, Sweden.

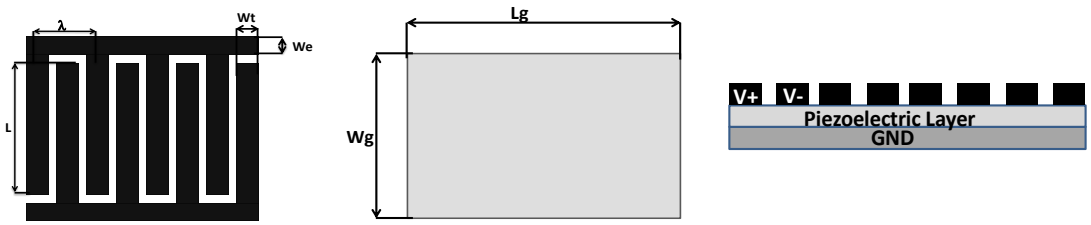

Figure 1. Structure of the single sided IDT transducer (top electrode, bottom electrode, cross-section)

Single sided IDT

Interdigital transducers have been used for generating surface acoustic waves in signal processing applications for a long time but their use in the NDT and SHM applications is relatively recent [1,7,4]. A typical IDT is built of three main layers: bottom (ground) electrode, piezoelectric layer (substrate), and top (phase) electrodes (Fig.1.) Bottom electrode is usually a plate that covers almost the whole bottom surface of the transducer. Top electrodes are formed in the comb/finger shapes. The distance between the electrodes (finger separation) defines the length of the generated wave [7,8]. The piezoelectric layer may be made of different materials: piezoelectric polymer (i.e., PVDF [9]), piezoceramics [10] or piezoceramic composites (i.e., MFC [1,7,11]). The type of substrate used defines different transducer properties, like its elasticity and maximal energy of the generated waves.
A very essential advantage of IDT transducers, besides their modal sensitivity, is their ability to generate narrow wave beams [12]. Signal is generated in the direction perpendicular to the finger electrodes and the beam pattern divergence depends on the fingers length. Inherent IDT directivity can be even improved by the use of an anisotropic piezoelectric substrate like MFC.

Double sided IDT

In the traditional design of the IDT, only one side of the transducer is covered by the interdigital electrodes while the other side is made as a plain electrode. In such a design three electrical connections are required: two for the two sets of interdigital electrodes and one for the ground electrode. Double sided IDT has the interdigital electrodes formed on both sides of the transducer. In this case there are two sets of finger electrodes at the same position (one on the top surface, other on the bottom surface), which results in four comb electrodes. To simplify wiring the top and bottom electrodes are connected in pairs so that the opposite phase electrodes are placed over each other (Fig.2).

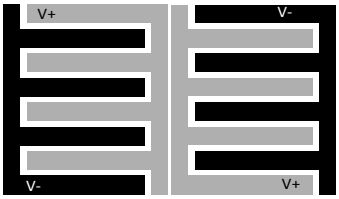

Figure 2. Electrode layout in the double sided IDT (top electrode-left, bottom electrode-right)

DESIGN PROCESS OF THE INTERDIGITAL TRANSDUCER

The IDTs presented in this paper are designed to excite the A0 mode in a 4mm thick aluminum plate. This mode exists at a broad band of frequencies, however, the most useful for the SHM applications are the frequencies characterized by low dispersion, i.e., the frequency band for which the excited waves travel with approximately the same speed. This situation occurs at the points where group velocity reaches its extreme at the dispersion plot (Fig. 3). In our case, the maximum of the group velocity of the A0 mode in a 4mm thick aluminum plate exists at 329 kHz, and this frequency has been chosen for our IDT design. Phase velocity for given frequency may be read from the dispersion curves in Fig. 4.
Wavelength of the desired Lamb wave is defined as:

$$\lambda = \frac{C_p}{f} = 7{,}5mm \tag{1}$$

where C_p is the phase velocity and f is the frequency.
The layout of the designed electrodes is presented in Fig. 5 (right) for the single sided (SS) IDT, and fig 5 (left) for the double sided (DS) IDT; the respective dimensions are in Table I.

Table. I. Dimensions of the designed interdigital transducers (Fig.1)

	λ [mm]	L [mm]	Wt [mm]	We [mm]	Lg [mm]	Wg [mm]
SS IDT	*7.5*	*15*	*1.9*	*0.75*	*28.2*	*15*
DS IDT	*7.5*	*15*	*1.9*	*0.75*	---	--

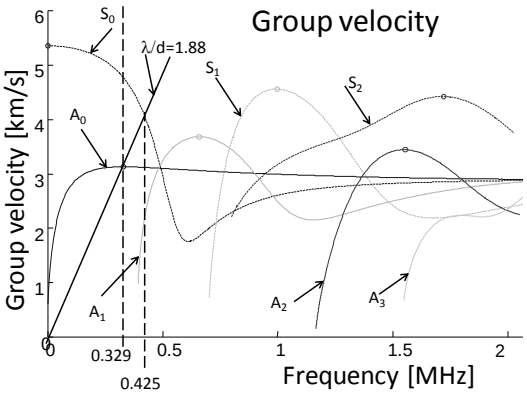

Figure 3. Group velocity for a 4 mm aluminum plate.

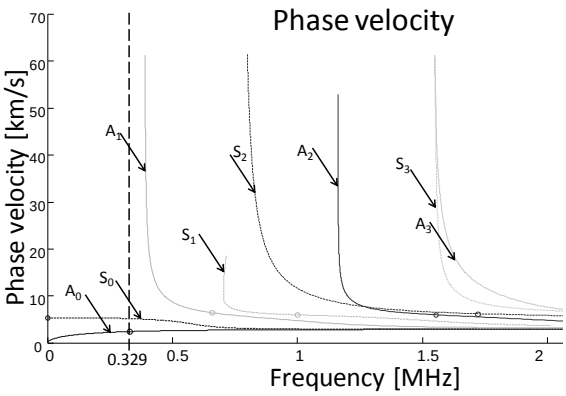

Figure 4. Phase velocity for a 4 mm aluminum plate.

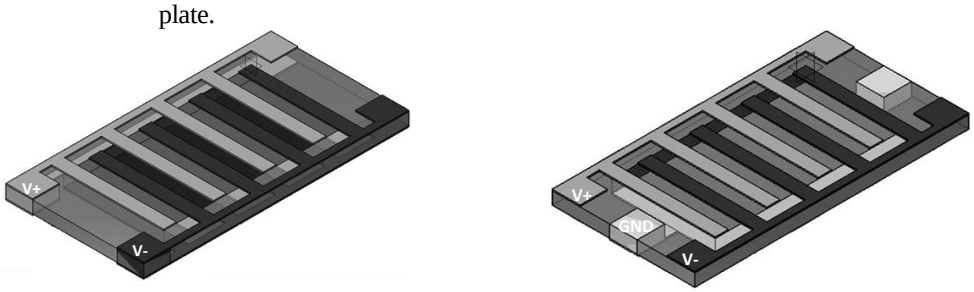

Figure 5. The designed IDT (double side-left, single side-right).

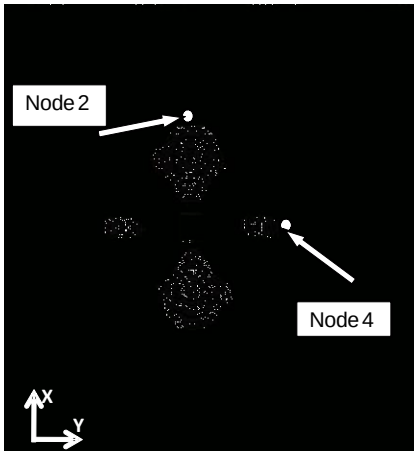

Figure 6. Localization of the measuring points during the simulations.

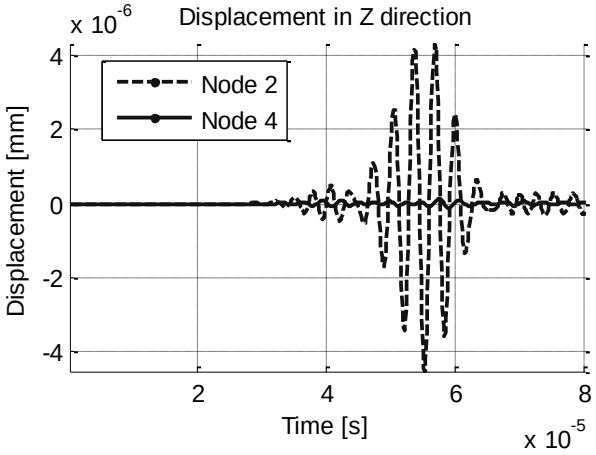

Figure 7. Out of plane displacements acquired during the simulations at Node 2 and Node 4

NUMERICAL SIMULATIONS

Numerical model of the IDT transducer located centrally on a 4mm thick aluminum plate with dimensions 500x500 mm was created in ANSYS Multiphysics software. The structure model was built using 20-node "brick" elements in finite element analysis (FEA). Fully coupled transient analysis was performed to simulate the piezoelectric effect of the IDT transducer. All simulations were performed with the same settings; transducers were excited with the same electrical signals (five-cycle tone burst modulated with Hanning window, amplitude $100V_{p\text{-}p}$); simulation time was $80\mu s$.

Single sided IDT

During simulations of the single sided IDT two measuring points were located on the plane at the distance of 250mm from the center of the plane, one in the X-direction and the second in the Y-direction (Fig. 6). Vibration amplitude was measured both in the in-plane and out-of-plane directions. In both cases amplitude of the generated waves in Node 4 was ten times lower than in Node 2 (Fig.7). Therefore for further analysis only data from the Node 2 is used.

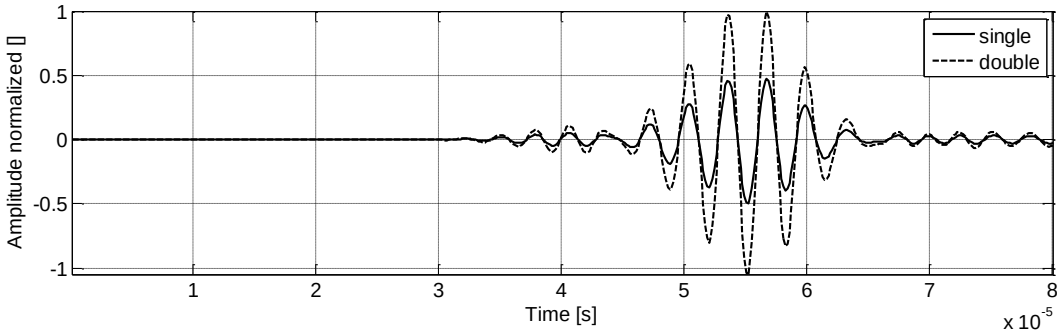

Figure 8. Time plots of the out-of-plane vibrations obtained during FEA simulations of IDT.

Double sided IDT

The second set of simulations was performed to compare amplitudes and spectra of the snapshots generated by the single- and double-sided IDTs. The main difference in the simulation results is the difference in amplitude of the waves generated by the two types of the transducers (Fig. 8). The double-sided transducer generates a wave with amplitude 2.1 times higher than that obtained during the simulations of the single-sided transducer. Moreover, the second set of electrodes does not only increase amplitude of the generated waves but also simplifies the power supply system. This is possible since it has only two sets of electrodes ("positive" and "negative") instead of three sets of the electrodes ("positive', "negative" and "ground").

EXPERIMENTAL RESULTS

A series of experimental tests has been performed to verify the numerical results of the designed transducers. The following properties of the transducers have been investigated during the experiments:

- Frequency spectrum of the generated wave for the nominal excitation frequency,
- Influence of the excitation frequency on amplitude of the generated wave,
- Directionality of the generated wave for the nominal frequency.

The designed IDT was mounted on a 4mm thick, 1000x1000 mm aluminum plate with Loctite 3450 epoxy bond which had been cured for at least 24h before tests. The excitation signal was generated by the Piezo Acquisition System PAS-8000 and PAQ-16000D from EC-Electronics, Poland. Polytec PSV-400 scanning laser vibrometer was used for the vibration measurements (Fig. 9). Laser vibrometer was located at the distance of 1302 mm in front of the scanned plate. To improve reflective properties of the surface, the measured area was covered with retro-reflecting material dedicated for the laser vibrometry tests. The measurements were performed using sampling frequency 5.12 MHz, and the sensitivity was set on 20mm/s/V. To suppress the measurement noise each measurement was repeated 8 times and the results were averaged. The excitation signal used in the experiment was the same as that during simulations. The excitation frequency during the point measurements was varied from 100 to 500 kHz in 50 kHz steps; additional frequencies were used in the vicinity of the nominal frequency, i.e., 330, 375 and 425 kHz. Beam pattern of the generated GW was tested in the measurement points shown in Fig. 10 for the excitation frequency 330 kHz.

Single sided IDT

The snapshots collected for the points V3 and H4 during the experiment with the nominal excitation frequency of 330 kHz are presented in Fig. 11. From Fig. 11 can be seen that the experimentally measured amplitude of the waves generated in front of the transducer (V3 point) is an order higher than that of side waves (H4 point), which agrees with the simulation result. Frequency analysis of the snapshot measured at V3

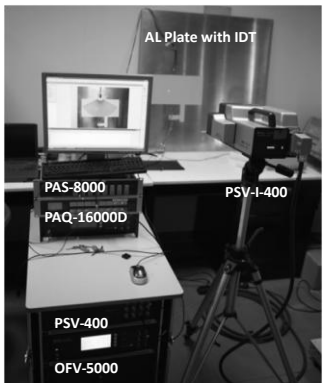

Figure 9. Experimental set up used to test designed transducers

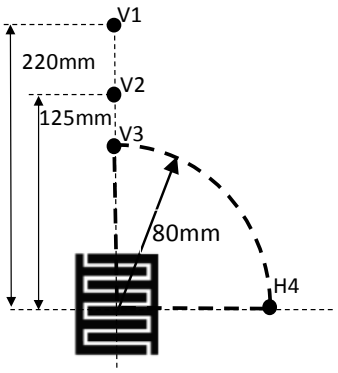

Figure 10. Location of the sensors and measuring points during the experiments.

shows that the IDT generated a narrow band signal with the same center frequency as the excitation frequency (see Fig. 12). Additional weak peaks are also visible in the vicinity of 430 and 490 kHz. These frequencies have been identified as the S0 mode frequency (425 kHz) and the electrical resonance (490 kHz). In the H4 measurements these frequencies are also visible but the 330 kHz frequency is not the dominating one. Change of the excitation frequency not only changes the frequency spectrum but also influences the amplitude of the excited wave, which can be seen in Fig. 13 where amplitudes of the generated waves are shown as a function of frequency.

It is apparent that the "side" wave (H4-point) has much lower amplitude than the "front" one, especially in the vicinity of the nominal and resonant frequencies. For frequencies much higher than the nominal one the amplitudes increase slowly when approaching the resonant frequency.

To determine the beam pattern of the generated waves point measurements were performed in a number of points on a quarter of circle with diameter of 80 mm (Fig. 10). These measurements also confirmed the result the point measurements presented above, i.e., that amplitude of the "front" waves is considerably higher than that of the "side" wave. The "front" wave takes the form of a lobe with width of +/- 23º from the IDT's symmetry axis (see Fig. 15).

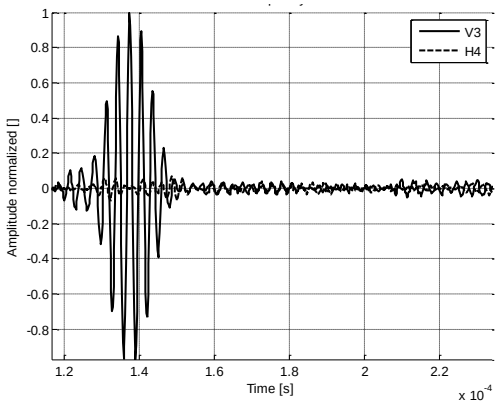

Figure 11. Time plot of the measured signal

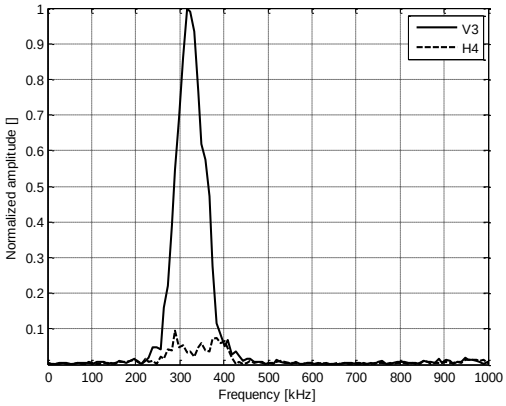

Figure 12. Frequency spectrum of the snapshot.

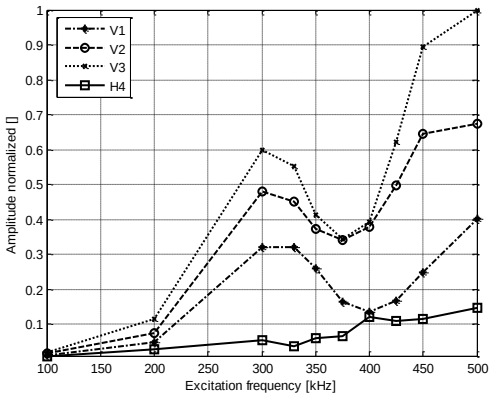

Figure 13. Maxima of the GW: SS-IDT

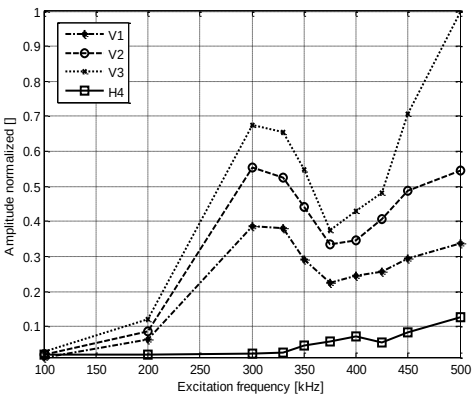

Figure 14. Maxima of the GW: DS-IDT

Double sided IDT

Experimental results obtained during the tests of the double sided IDT also clearly indicate the directionality of the generated wave as shown in Fig. 14 presenting the snapshots frequency spectra. The maximum snapshot amplitude at the front of the IDT (V-points) increases with frequency until nominal frequency of the transducer is reached. Further increase of the excitation frequency leads to a rapid reduction of the observed amplitude and then amplitude starts rising again above 400 kHz to reach its maximum around the resonance frequency at 490 kHz. Variation in the excitation frequency has minimal influence on the amplitude of the excited side waves below the nominal frequency. Further increase of the frequency results in the sudden drop and then followed by a rise of the H-point amplitude to the global maximum at 490 kHz.
The waves generated by the double sided IDT have spatial characteristics similar to that of the single sided – the main lobe is formed in front of the transducer, its width is approx. +/- 25º from its main axis (see Fig. 16).

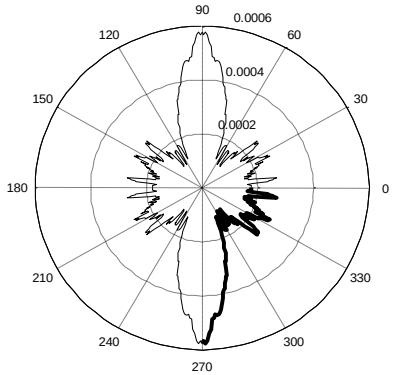

Figure 15. Beam pattern of single sided IDT

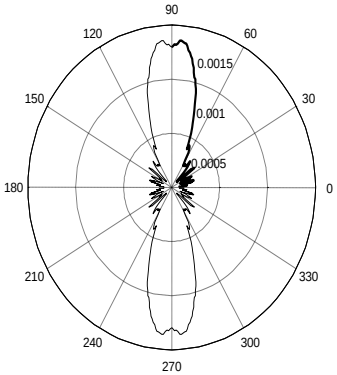

Figure 16. Beam pattern of double sided IDT

CONCLUSSIONS

Novel design of interdigital transducer based on macro-fiber piezocomposite was presented in the paper. Two alternative designs were investigated: the single- and double-sided IDT. Numerical and experimental results confirmed that the transducer is characterized by modal selectivity and highly directional beam pattern.
Comparison between single- and double-sided transducer clearly indicates that main difference between those types of IDT is amplitude of the generated "front" wave. Adding second set of interdigital electrodes in the double-sided design leads to doubling of the "front" wave amplitude with the "side" wave amplitude reaming at the same level as for the single-sided design.
Increased "front" wave amplitude and simpler wiring makes the double-sided interdigital transducer more feasible solution for the SHM applications.

REFERENCES

1. Raghavan, A.; Cesnik, C. E. S. Review of Guided-wave Structural Health Monitoring. *The shock and vibration digest*,39(2), pp. 91-114, March 2007.
2. Culshaw, B.; Pierce, S. G.; Staszewski, W. J. Condition monitoring in composite materials: an integrated systems approach. *Proceedings of Institute of Mechanical Engineers*, no. 212, pp.189-201, 1998.
3. Ghosh, T.; Kundu, T.; Karpur, P. Efficient use of Lamb modes for detecting defects in large plates. *Ultrasonics*, no. 36, pp. 791-801, 1998.
4. Salas, K. I.; Cesnik, C. E. S. Design and Characterization of the CLoVER Transducer for Structural Health Monitoring. *Procedings of SPIE*. Vol 693. 2008.
5. Salas, K. I.; Cesnik, C. E. S. Guided wave excitation by a CLoVER transducer for structural health monitoring: theory and experiments. *Smart Material and Structures*, no. 18, 2009.
6. Rose, J. L. A baseline and vision of ultrasonic wave inspection potential. *Journal of pressure vessel technology*, no. 124, pp. 273-282, 2002.
7. Monkhouse, R. S. C.; Wilcox, P. D.; Cawley, P. Flexible interdigital PVDF transducers for the generation of Lamb waves in structures. *Ultrasonics*, no. 35, pp. 489-498, 1997.
8. Monkhouse, R. S. C. et al. The rapid monitoring of structures using interdigital Lamb. *Smart Materials and Structures*, no. 9, pp. 304-309, 2000.
9. Wilcox, P. D.; Cawley, P.; Lowe, M. J. S. Acoustic fields from PVDF interdigital transducers. *IEE Proceedings Science, Measurement and Technology*, 145(5), 1998.
10. Luginbuhl, P.; Collins, S. D.; Racine, G.; Gretillat, M. A.; de Rooij, N. F.; Brooks, K. G.; Setter, N., Microfabricated Lamb Wave Device Based on PZT Sol-Gel Thin Film for Mechanical Transport of Solid Particles and Liquids. *Journal Of Microelectromechanical Systems*, vol. 6, no. 4, pp. 337-346, 1997.
11. Williams, B. R.; Park, G.; Inman, D. J.; Wilkie, K. W.An Overview of Composite Actuators with Piezoceramic Fibers. *20th International Modal Analysis Conference*. Los Angeles. pp. 421-427, 2002.
12. Na, J. K.; Blackshire, J. L.; Kuhra, S. Design, fabrication and characterization of single-element interdigital transducers for NDT applications. *Sensors and Actuators A*, no. 148, pp. 359-365, 2008.